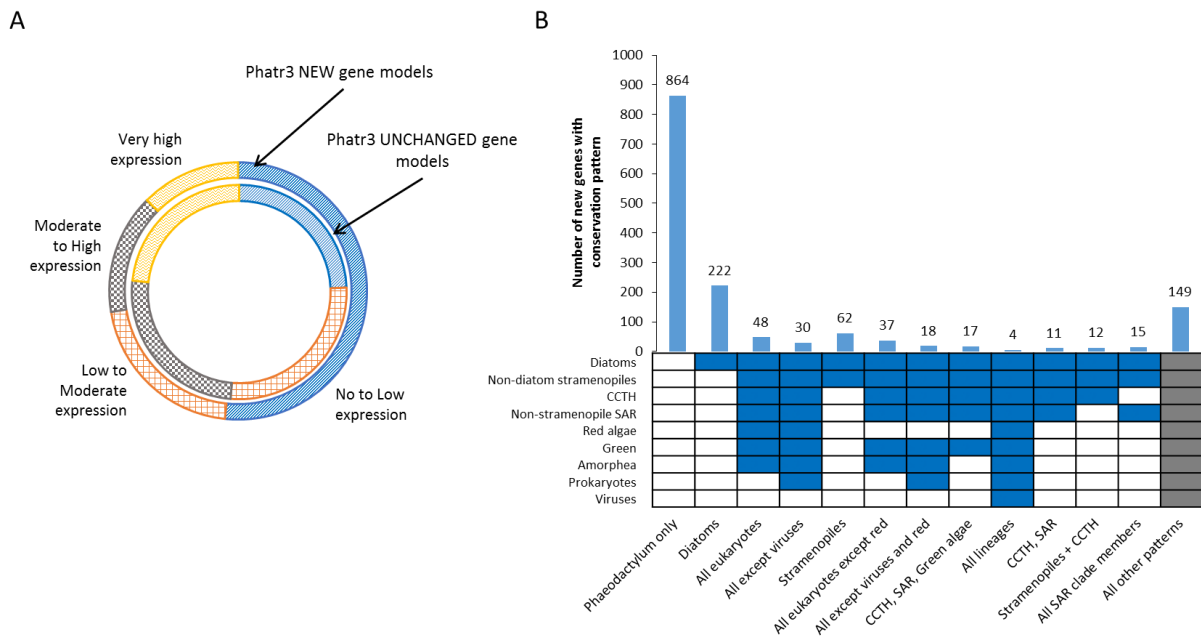


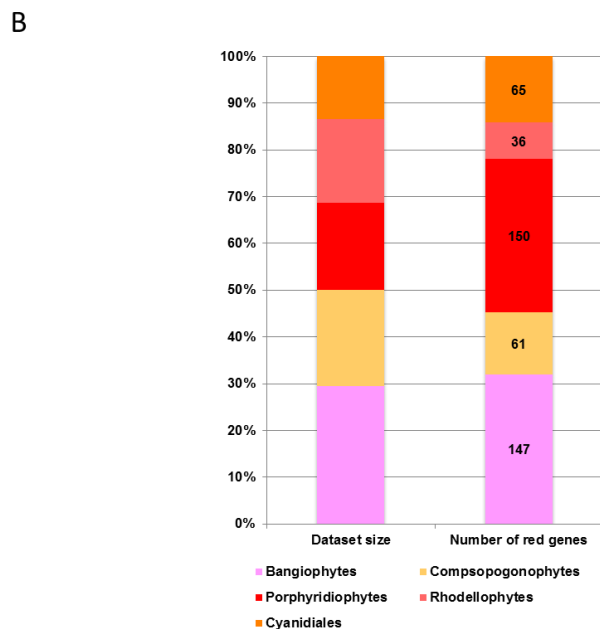
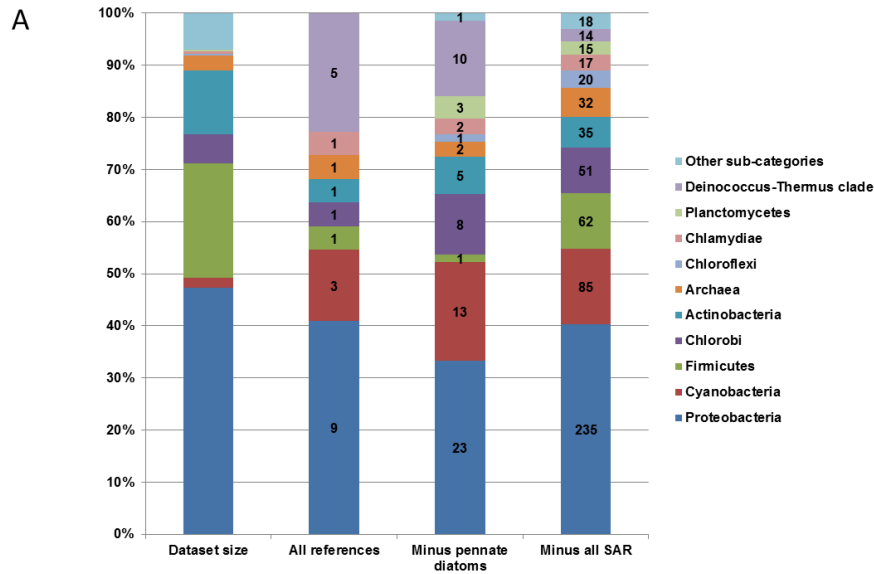
Integrative analysis of large scale transcriptome data draws a comprehensive landscape of *Phaeodactylum tricornutum* genome and evolutionary origin of diatoms

Achal Rastogi, Uma Maheswari, Richard G. Dorrell, Fabio Rocha Jimenez Vieira, Florian Maumus, Adam Kustka, James McCarthy, Andy E. Allen, Paul Kersey, Chris Bowler and Leila Tirichine

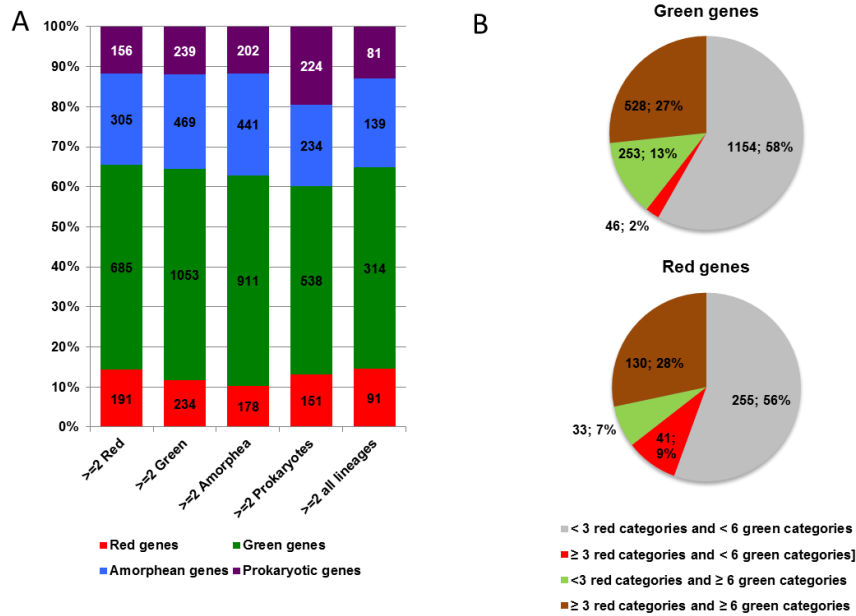
Supplementary Figures



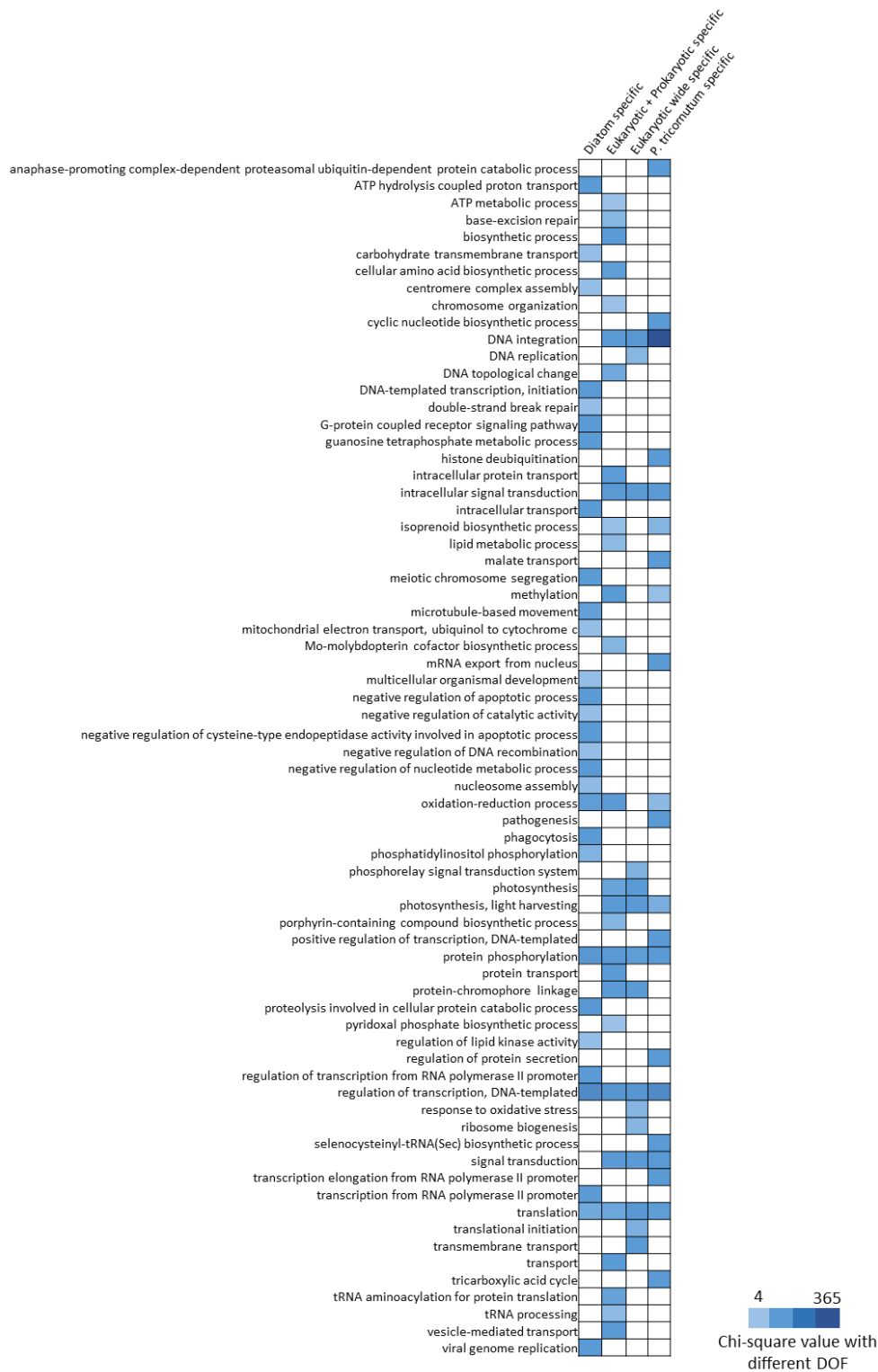
Supplementary Figure 1. Novel genes in Phatr3. (A) The circular stack plot represents the comparison of the expression profile between the proportion of novel Phatr3 gene models (outer circle) with that of the proportion of unchanged Phatr3 gene models (inner circle). (B) The heatmap and graph are shown as per Fig 1.



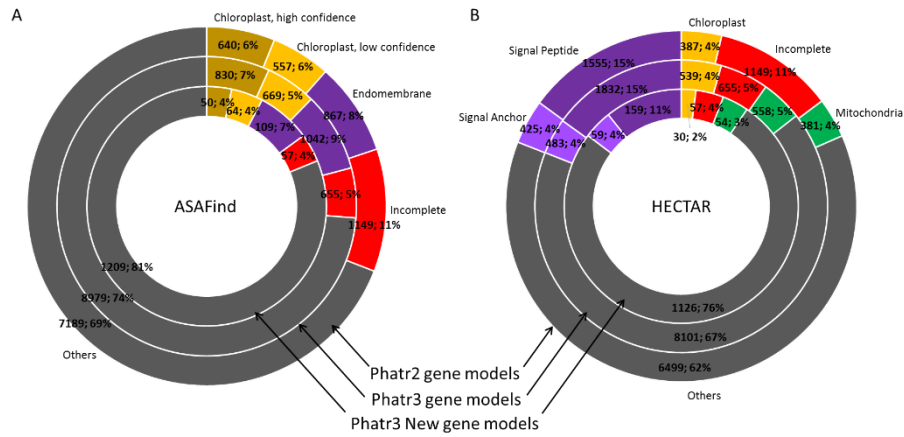
Supplementary Figure 2. Specific taxonomic affiliations of Prokaryotic, Red and Green genes. Each chart shows the specific sub-category from which different prokaryotic (A), and red (B) genes arose. All genes that were assigned (i.e., two or more top hits from two or more sub-categories from a particular lineage, prior to the first top hit from outside that lineage) using the most reduced reference dataset (i.e., all reference sequences, excluding SAR clade members, and other algal lineages with secondary or tertiary plastids) is shown. For prokaryotic genes, two other distributions (obtained for the entire dataset minus non-ochrophyte algae with secondary or tertiary plastids, and the entire dataset minus pennate diatoms, and all non-ochrophyte algae with secondary or tertiary plastids) are shown. Each chart additionally shows the relative size of each sub-category within the reference sequence library, demonstrating that certain sub-categories contribute to substantially more of the top hits (e.g., the *Deinococcus-Thermus* clade in the distribution of prokaryotic genes for the full and pennate diatom-free datasets that were modified to remove all non-ochrophyte lineages with secondary or tertiary plastids) or fewer of the top hits (e.g., the streptophytes, in the distribution of green genes for the dataset from which all SAR clade sequences, and other non-ochrophyte lineages with secondary or tertiary plastids were removed) than might be expected given the corresponding dataset size.



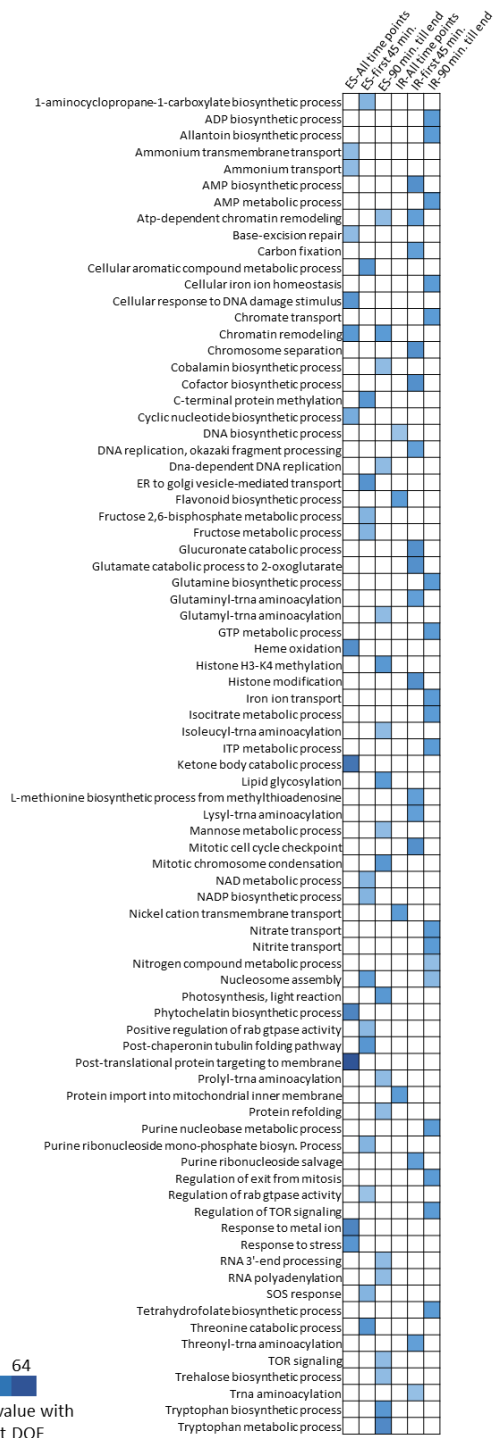
Supplementary Figure 3. Green genes are not purely a result of taxonomic undersampling or lineage-specific gene loss. (A) shows the taxonomic affiliations of genes identified by BLAST top hit analysis, with the dataset from which all SAR clade sequences, and other non-ochrophyte lineages with secondary or tertiary plastids were removed, for which orthologues could be identified in at least two red, green, amorphean or prokaryotic sub-categories, and for which orthologues could be identified in at least two each of the red, green, amorphean and prokaryotic sub-categories. In each case, substantially more genes of green affinity were identified than of other taxonomic affiliation. (B) Compares the number of genes of red or green taxonomic affiliation for which RbH orthologues could be identified in a majority of red (3/5) or green (6/11) sub-categories. A similar proportion of genes of inferred red origin (130/459, 28%) and genes of inferred green origin (528/ 1,981, 27%) were found to have orthologues in a majority of both red and green sub-categories, indicating that the identification of green genes within the dataset was not unfairly biased by taxonomic undersampling of red lineages.



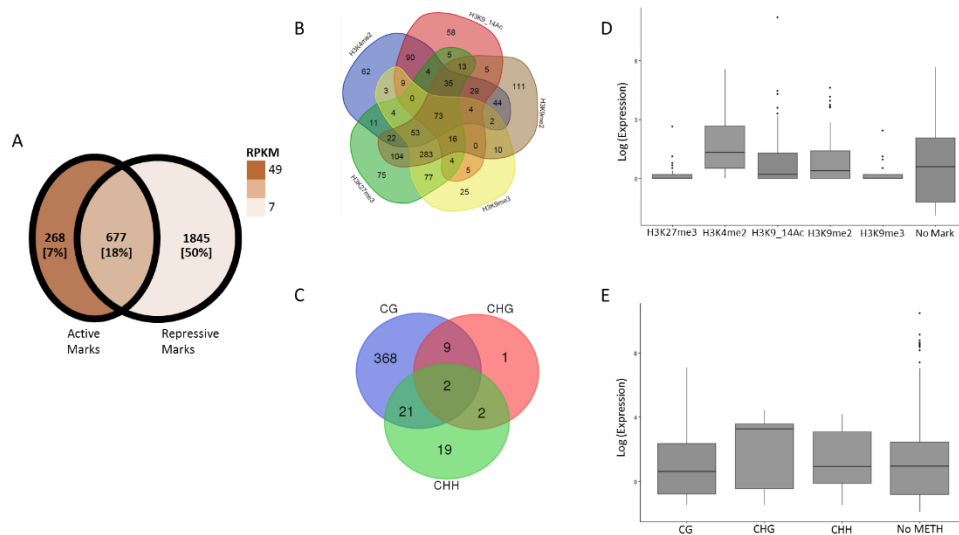
Supplementary Figure 4. Enrichment of biological processes within genes identified to be specific to different groups of organisms. The heat map, indicating chi-square values which are significant (P -value < 0.05) with different degrees of freedom (DOF), depicts various biological processes (left Y-axis) that are enriched in the pool of genes found specific to different groups of organisms (top X-axis). Chi-square values are used to rank the most significant biological processes in descending order. High chi-square value here indicates higher significance (very low P -value) compared to low chi-square values indicating higher P -value but < 0.05 .



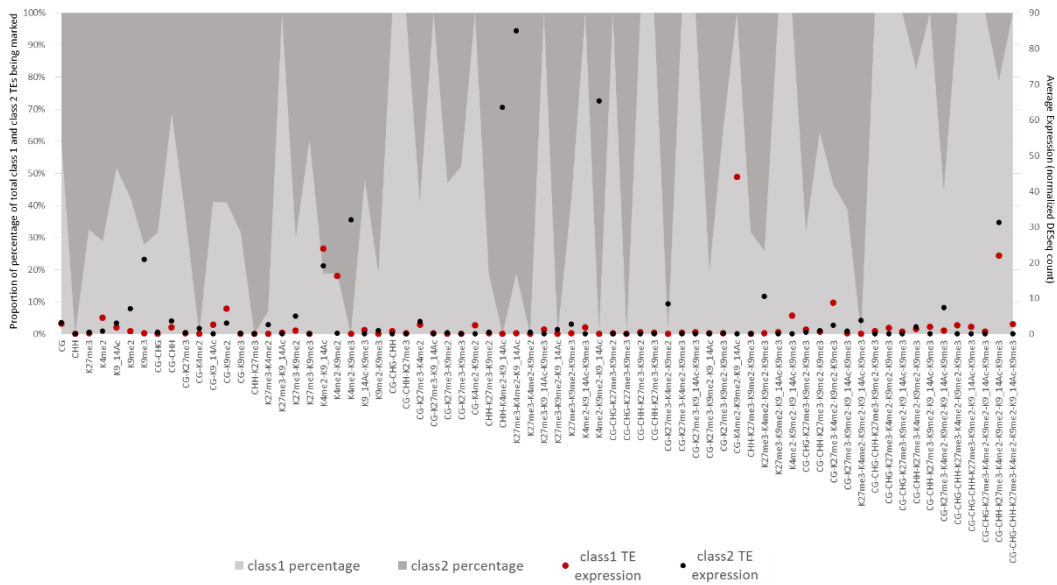
Supplementary Figure 5. Predicted subcellular localization of *P. tricornutum* proteins. This figure shows the targeting predictions for proteins encoded within the *P. tricornutum* genome as assessed using the diatom targeting predictor programmes (A) ASAFind (Gruber et al., 2015) and (B) HECTAR (Gschoessl et al., 2008). The figure is in accordance with Figure 3 panel A and B.



Supplementary Figure 6. Enrichment of biological processes within genes exhibiting alternative splicing at various time-points under Nfree culture conditions. The heat map, indicating chi-square values which are significant (P -value < 0.05) with different degrees of freedom, depicts various biological processes (left Y-axis) that are enriched in the pool of genes exhibiting alternative splicing in the context of intron-retention and exon-skipping (top X-axis). The figure is in relation with categories represented in Figure 4 panel C. Chi-square values are used to rank the most significant biological processes in descending order. High chi-square value here indicates higher significance (very low P -value) compared to low chi-square values indicating higher P -value but < 0.05 .



Supplementary Figure 7. Distribution of epigenetic modifications over transposable elements. The Venn diagram (A) represents different chromatin states maintained based on the association of TEs with repressive, active or both repressive and active chromatin modifiers. Numbers and percentages in the Venn diagram reflects the absolute number of TEs and the relative percentage out of the total Phatr3 TEs. The Venn diagram in (B) presents the number of new TEs found to be localized by one or more histone H3 PTMs, and (C) presents the new TEs methylated in different context (CG, CHH, and CHG) of DNA methylation. Boxplots (D) and (E) represents average (median) expression of genes marked exclusively either of the H3 PTMs and are DNA methylated in either of the context, respectively, in normal condition.



Supplementary Figure 8. Epigenetic marking over transposable elements. The area plot represents the proportion of Class I vs Class II transposable elements being marked by different epigenetic marks including Histone H3 post-translational modifications and DNA methylation (CG, CHH and CHG). Black and red dots indicate the average RNA expression of all the TEs (wherever available) marked in different contexts.

BLAST results obtained using	i) Monophyly of ochrophytes			ii) Sister-group to ochrophytes		
	All data	All except pennate diatoms	All except diatoms	All except ochrophytes	All except stramenopiles	All except SAR
1) BLAST and single-gene tree data comparable						
BLAST and tree topologies congruent	322	314	302	114	109	114
BLAST and tree topologies not congruent	0	0	2	35	35	34
% tree and BLAST topologies congruent	100	100	99.3	76.5	75.7	77.0
2) BLAST and single-gene tree data not comparable						
Not comparable to BLAST- BLAST data insufficiently resolved	2	10	20	141	133	127
Not comparable to tree- topology ambiguous	0	0	0	30	37	39
Not comparable to tree- outgroup sequences not incorporated into tree	0	0	0	4	4	4
Not comparable to tree- sister-group excluded from BLAST analysis	0	0	0	0	6	6

Supplementary Figure 9. Verification of the reconstruction of evolutionary origins by BLAST top hit analysis. (A) Compares the results of BLAST top hit analysis and single-gene phylogeny for 324 genes in Phatr3 incorporated into an independent phylogenetic study of plastid-targeted proteins with broad ochrophyte distribution¹⁰. Each of the proteins incorporated are found to produce a monophyletic or paraphyletic ochrophyte clade, i.e., should produce BLAST top hits to diatom or other ochrophyte sub-categories in the raw BLAST top hit analysis, and in BLAST top hit analyses from which pennate diatoms and all diatoms have been removed (but other ochrophytes have been retained). In addition, each protein should have a similar BLAST top hit in analyses from which all ochrophyte, stramenopile or SAR clade sequences have been removed to the sister-group to the ochrophyte clade (either red algae, green algae, aplastidic stramenopiles, other eukaryotic lineages, or prokaryotes) inferred from the single-gene tree. The overwhelming majority of the BLAST top hit analyses support monophyly of the ochrophytes, and at least three quarters retrieve the same ochrophyte sister-group as determined through single-gene tree analysis.

Supplementary Table Legends

Supplementary Table 1. The Supplementary File summarizes the findings of the paper in a more holistic view

Supplementary Table 2. Reciprocal best BLAST hit analysis of gene sharing between *Phaeodactylum tricornutum* and other organisms.

Supplementary Table 3. BLAST top hit analysis of gene origin from *Phaeodactylum tricornutum* and multiple reference sequence libraries, excluding non-ochrophyte sub-categories with secondary or tertiary plastids.

Supplementary Table 4. Taxonomic sub-divisions used when constructing the multi-sequence reference library.

Supplementary Table 5. Enriched biological process within genes identified to be specific to different groups of organisms.

Supplementary Table 6. Sub-cellular localization output from ASAFind and HECTAR, analyzed over the entire Phatr3 genes and Phatr3-JGI gene models.

Supplementary Table 7. The file describes all the biological processes which are significantly enriched within genes exhibiting alternative splicing (exon-skipping/intron retention) at different time-points of Nfree culture conditions, compared to all processes Phatr3 annotations.

Supplementary Table 8. File listing the structural and functional annotations of Phatr3 transposable elements (TEs).

Supplementary Table 9. Illumina RNA-Seq libraries used for Phatr3 annotations.

Supplementary Table 10. BLAST top hit analysis of gene origin from *Phaeodactylum tricornutum* and multiple reference sequence libraries.

Supplementary Table 11. Phylip format trimmed alignments, and nexus format tree outputs for each phylogeny

Other Supplementary File Legends

Supplementary File 1. Comparison of certain Phatr3 gene structure with that of Phatr2.

Supplementary File 2. The description of the taxonomic divisions.

Supplementary File 3. Exemplar phylogenetic trees concordant with the BLAST top hit analysis.

This figure presents trees of eight genes within the *P. tricornutum* genome, which encode plastid-targeted proteins with broad evolutionary conservation across the ochrophytes, and a deeper ultimate evolutionary origin involving horizontal transfer from prokaryotes, red or green algae¹⁰. Trees were calculated from manually curated alignments, using MrBayes and RAxML, under three different substitution matrices (GTR, Jones/JTT, and WAG). The first sheet ("Overview") provides **i**) details of each gene alignment, the tree topology obtained, and compares this to the BLAST output obtained for that gene with the dataset from which all lineages with a suspected history of secondary endosymbiosis were removed, and **ii**) a legend showing the ways in which taxonomic identity and support values are presented in each tree.

The remaining sheets present outputs for each tree. Sheets **A-C** present three trees for genes of ultimate prokaryotic origin: **A** shows an exemplar gene (plastid pyruvate kinase) with limited direct homology outside of the ochrophytes and prokaryotes; and **B-C** show two genes (plastid beta-ketoacyl synthase, and ribulose-5-phosphate 3-epimerase) in which ochrophyte, haptophyte and cryptomonad sequences are more closely related to prokaryotic lineages (respectively chlamydiobacteria and proteobacteria) than other eukaryotes. Sheets **D-E** present two exemplar genes (dual plastid-mitochondrial prolyl tRNA-synthetase, and a periplastid-targeted Mpv17 protein) with deeper red algal affinity. In each case, the ochrophyte, haptophyte and cryptomonad sequences resolve with red algae to the exclusion of aplastidic members of the SAR and CCTH clades (e.g. oomycetes), consistent with a late acquisition of the ochrophyte plastid. Sheets **F-H** present two exemplar genes (plastid DAHP synthetase, and glutathione S-transferase) for which ochrophyte, haptophyte and cryptomonad sequences resolve at specific points within the chlorophyte lineages (respectively Dolichomastigales, and members of the mamiellophytes), and one tree (plastid cyloeucanol cycloisomerase) that posits a deep origin for the ochrophyte sequences within the chlorophyte algae. The presence of red algal orthologues in each tree confirms these genes are not misidentified as a result of undersampling of red lineages, and the evolutionary relationship of these genes to chlorophytes, to the exclusion of streptophyte lineages, indicates a probable horizontal transfer event, as opposed to shared inheritance and differential loss.

Supplementary File 4. EOULSAN parameter Supplementary File specifying the parameters used to analyze the expression using RNA sequencing libraries.

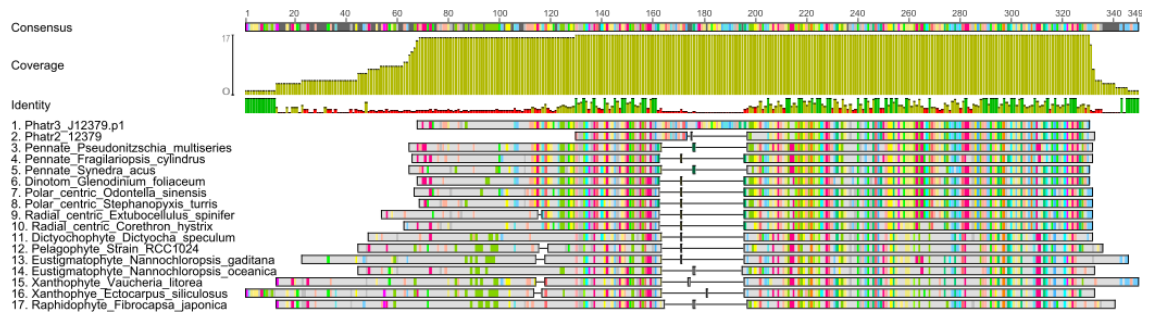
Full list of conserved plastid-targeted proteins identified de novo by Phat3. This lists all of the proteins that have been demonstrated in a separate study (Dorrell et al., manuscript submitted) to form conserved components of the ochrophyte plastid proteome, for which the gene model in Phatr3 encodes a predicted plastid-targeted protein (as inferred either with HECTAR or with ASAFind), and the gene model in Phatr2 is N-incomplete. In each case, the protein cluster identifier (as supplied in Dorrell et al.), functional annotation, and gene ID of each protein in Phat2 and Phat3 are provided.

Identifier	Function	Phat2	Phat3
2gh	SAM (and some other nucleotide) binding motif	Phatr2_4846	Phatr3_J4846
2jh	Fatty acid desaturase 4	Phatr2_5271	Phatr3_J5271
2kr	Heme oxygenase	Phatr2_5851	Phatr3_J5851
2ks	Heme oxygenase	Phatr2_5902	Phatr3_J5902
2kw	CDP-alcohol phosphatidyltransferase/ Phosphatidylglycerol-phosphate synthase	Phatr2_8663	Phatr3_J8663
2kx	Lycopene beta cyclase	Phatr2_8835	Phatr3_J8835
2la	Predicted unusual protein kinase	Phatr2_bd116	Phatr3_draftJ116
2lb	ATP-dependent Clp protease subunit	Phatr2_7525	Phatr3_draftJ263
2lc	CDGSH-type Zn-finger containing protein	Phatr2_bd297	Phatr3_draftJ297
2lt	Ferredoxin rieske component	Phatr2_9046	Phatr3_EG02174
2lv	Nitrite reductase	Phatr2_13154	Phatr3_EG02286
2lw	Ycf49-like protein	Phatr2_11197	Phatr3_EG02357
aav	Hypothetical protein	Phatr2_8324	Phatr3_J8324
xge	Retinol dehydrogenase	Phatr2_10567	Phatr3_J10567
xgj	Predicted unusual protein kinase	Phatr2_12121	Phatr3_J12121
xgn	Peroxisomal membrane protein MPV17 and related proteins	Phatr2_12379	Phatr3_J12379
xgo	FKBP-type peptidyl-prolyl cis-trans isomerase	Phatr2_12411	Phatr3_J12411
xgq	Alkyl hydroperoxide reductase, thiol specific antioxidant and related enzymes	Phatr2_12713	Phatr3_J12713
xgt	Uncharacterized conserved protein	Phatr2_13158	Phatr3_J13158
xgx	Serine O-acetyltransferase	Phatr2_13476	Phatr3_J13476
xhb	Peptide methionine sulfoxide reductase	Phatr2_14769	Phatr3_J14769
xhc	Predicted ATPase	Phatr2_1494	Phatr3_J1494
xhf	Seryl-tRNA synthetase	Phatr2_15374	Phatr3_J15374
xhg	Tryptophanyl-tRNA synthetase	Phatr2_15595	Phatr3_J15595
xhh	Glutathione S-transferase	Phatr2_15764	Phatr3_J15764
xhi	SsrA-binding protein	Phatr2_16021	Phatr3_J16021
xhn	tRNA uracil-5-methyltransferase and related tRNA-modifying enzymes	Phatr2_16911	Phatr3_J16911
xho	Glutaminyl-tRNA ligase	Phatr2_16963	Phatr3_J16963
xhp	RNA polymerase sigma factor	Phatr2_17029	Phatr3_J17029
xmv	Peptidase S41	Phatr2_3061	Phatr3_J3061

Comparative alignments of Phat2 and Phat3 conserved plastid-targeted proteins. This figure shows exemplar alignments of six proteins that are targeted to the plastids of a wide range of photosynthetic stramenopiles, for which the Phat2 gene model is incomplete at the N-terminus. For each protein, a global alignment of all stramenopile plastid-targeted sequences identified is shown (i), alongside close-up regions covering the N-termini (ii) of the Phat3 (iia) and Phat2 (iib) gene models. In each case the N-terminus identified by Phat3 broadly matches the N-terminus identified in orthologues from other stramenopile lineages, whereas the N-terminus identified by Phat2 is positioned within the conserved region of the protein. Otherwise conserved regions of sequence that are missing in Phat2 and completed by Phat3 are highlighted using coloured bars.

A) Mv22-type peroxisomal membrane protein

i) Full alignment

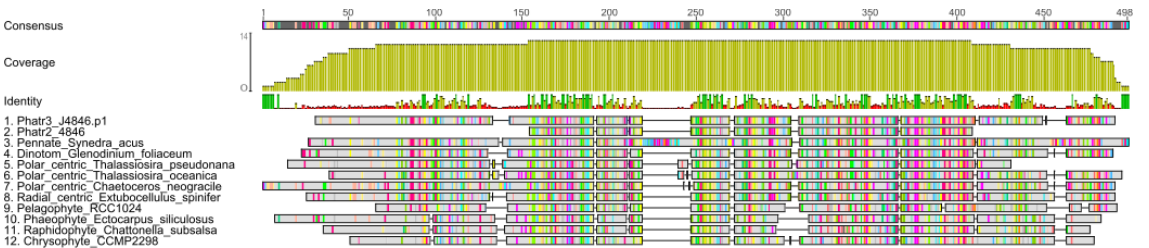


ii) N-terminus only

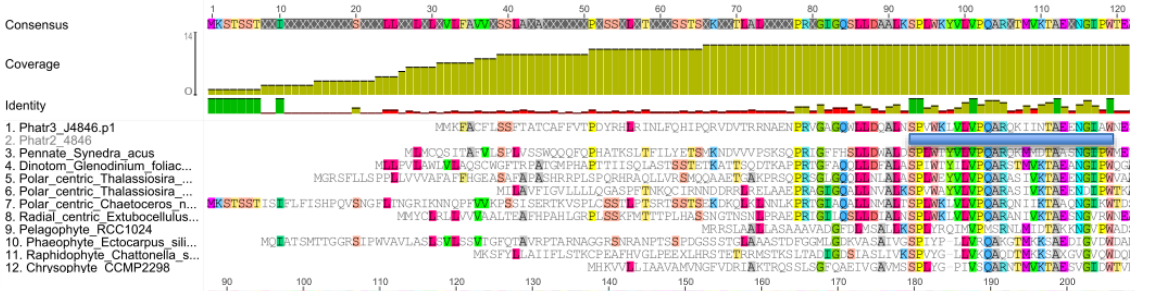


B) S-adenosyl methionine binding protein

i) Full alignment



iiia) Phat3 N-terminus

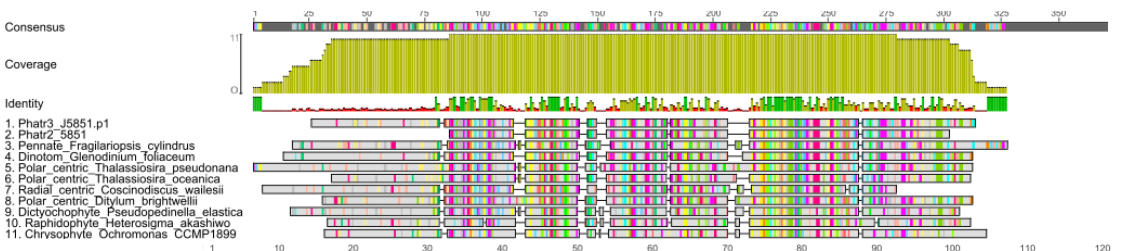


iiib) Phat2 N-terminus

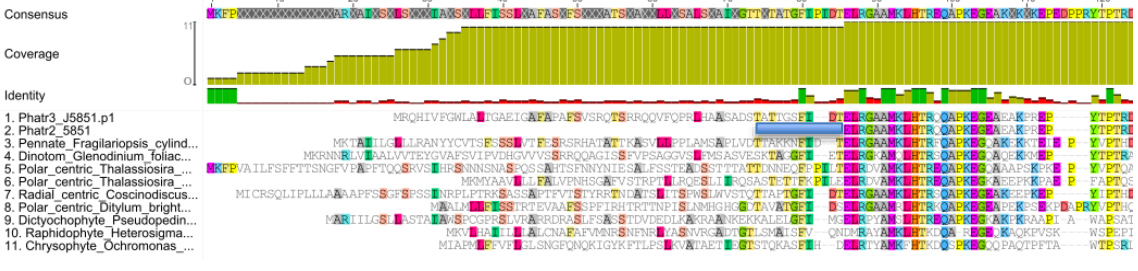


C) Phosphatidyl-glycerolphosphate synthase

i) Full alignment

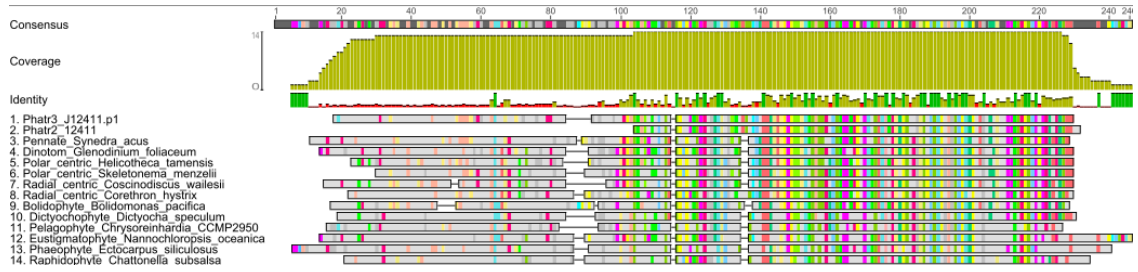


ii) N-terminus only

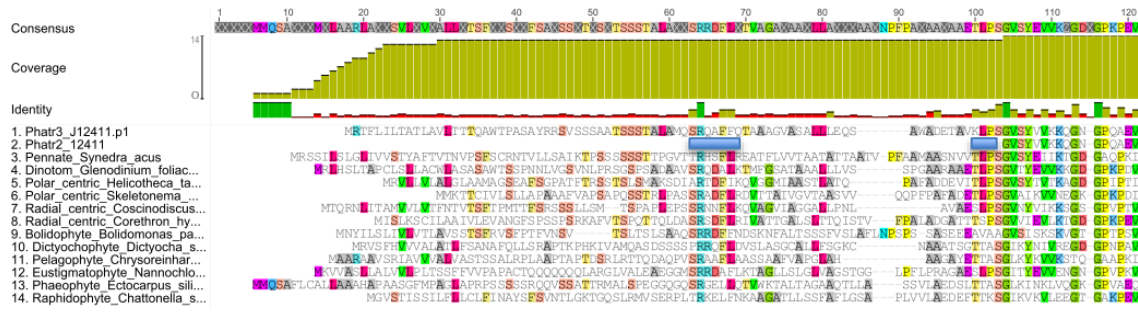


D) Peptidyl-prolyl cis-trans isomerase

i) Full alignment

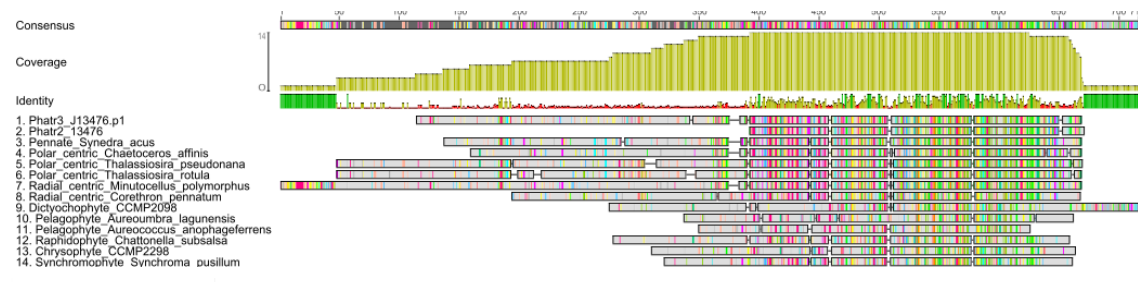


ii) N-terminus only

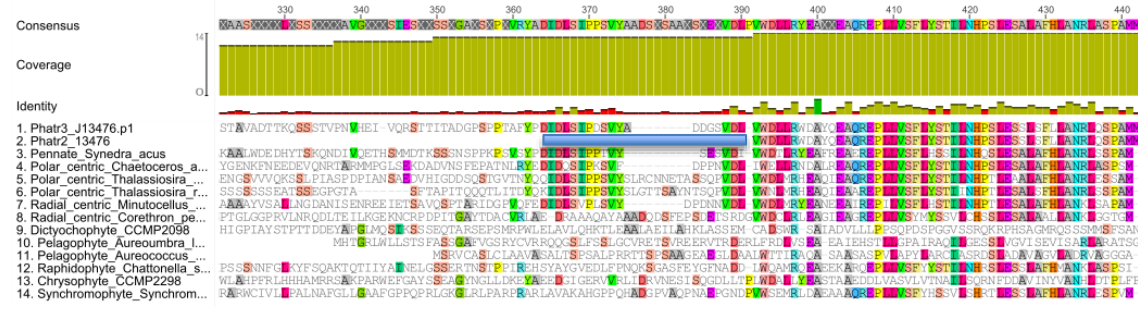


E) Serine O-acetyltransferase

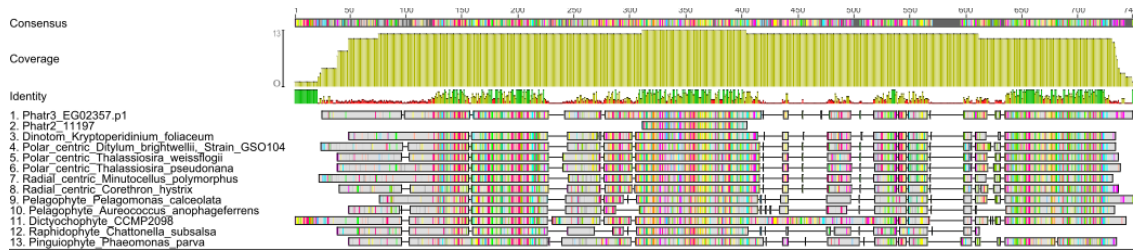
i) Full alignment



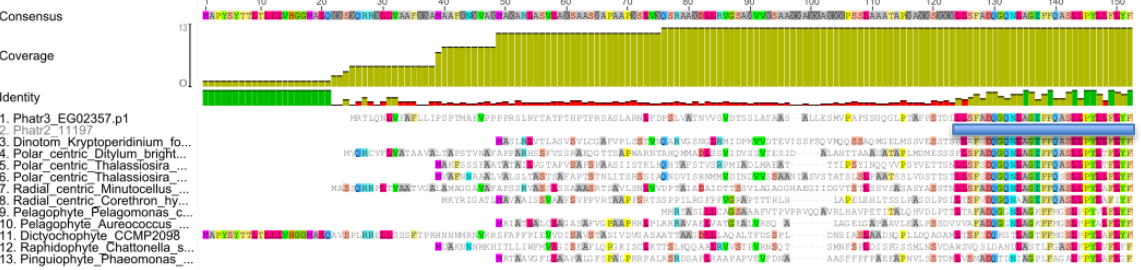
ii) N-terminus only



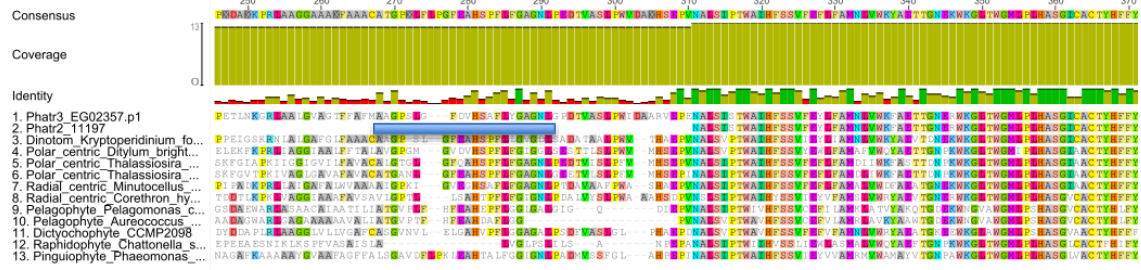
F) Ycf49-like protein



i) Full alignment



ii) Phat3 N-terminus



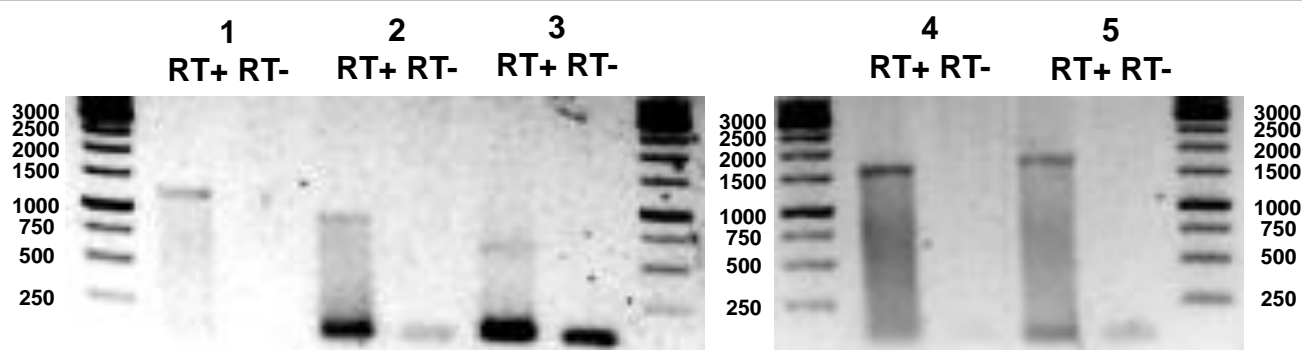
ii) Phat2 N-terminus

Exemplar RT-PCR of Phat3 conserved plastid-targeted proteins. Panel A tabulates the primers used for RT-PCR amplification of the five conserved plastid-targeted proteins identified specifically by Phat3 (Fig. SB), excluding the previously tested peroxisomal membrane-type protein. **Panel B** shows an exemplar gel photo, showing RT-PCR and cDNA negative control products for each gel. In each case the RT-PCR product gives a band of the expected size, whereas the cDNA negative control product does not. The molecular size standard used is GeneRuler 1 kb ladder (Thermo).

A)

Construct	Gene	PCR F	PCR R	mRNA length (nt)
1	S-adenosyl methionine binding protein	ATGATGAAATTTGCC TGTTTTTC	TTTTTTTTTATTTTCG AACAC	1206
2	Phosphatidyl-glycerolphosphate synthase	ATGACAGTGAATCGC CTTTTTTC	CTTACTGTTTGCTTT GAGTAG	897
3	Peptidyl-prolyl cis-trans isomerase	ATGCGTACCTTTCTG ATTC	ATCATCACCAATGAG TTCAATG	615
4	Serine O-acetyltransferase	ATGGTAGCGTGGCTC GTCCTGC	TATCCCGTCCGATTC AAACGTC	1620
5	Ycf49-like protein	ATGCGGACTTTGCAG AATCTG	CAGCTTTTTGACGGG TATAAC	1773

B)



Tree overview

i)

Panel	GeneID	Function	Matrix size (taxa x aa)	Tree topology	BLAST output (excluding other complex algal groups)
A	J22404	Plastid pyruvate kinase	55 x 421	Monophyletic group of ochrophytes and cryptomonads; sister-group to prokaryotes (eluisimicrobia)	Vertically inherited in ochrophytes; previously laterally acquired from prokaryotes (proteobacteria)
B	J37367	Plastid beta-ketoacyl synthase	76 x 405	Monophyletic group of ochrophytes, haptophytes and cryptomonads; sister-group to prokaryotes (chlamydiobacteria)	Vertically inherited in ochrophytes; previously laterally acquired from prokaryotes (chlamydiobacteria)
C	J53935	Plastid D-ribulose-5-phosphate 3-epimerase	70 x 223	Monophyletic group of ochrophytes and cryptomonads; sister-group to prokaryotes (proteobacteria)	Vertically inherited in ochrophytes; previously laterally acquired from prokaryotes (proteobacteria)
D	J43097	Plastid/mitochondrial prolyl-tRNA synthetase	99 x 493	Monophyletic group of ochrophytes, haptophytes, cryptomonads and red algae	Vertically inherited in ochrophytes; previously laterally acquired from red algae (porphyridiophytes)
E	J12379	Periplastid-targeted Mpv17 protein	104 x 185	Monophyletic group of ochrophytes, haptophytes and red algae	Vertically inherited in ochrophytes; previously laterally acquired from red algae (bangiophytes)
F	J24353	Plastid DAHP synthetase, class II	66 x 492	Monophyletic group of ochrophytes; sister-group to green algae (Dolichomastigales)	Vertically inherited in ochrophytes; previously laterally acquired green algae (streptophytes)
G	J45400	Plastid glutathione S-transferase	50 x 339	Paraphyletic group of ochrophytes, haptophytes and green algae (Pyramimonadales/ Mamiellophytes)	Vertically inherited in ochrophytes; previously laterally acquired green algae (Pyramimonadales)
H	J49447	Plastid cycloeucaanol cycloisomerase	55 x 292	Monophyletic group of ochrophytes, haptophytes and cryptomonads; sister-group to green algae (prasinophytes)	Vertically inherited in ochrophytes; previously laterally acquired green algae (Dolichomastigales)

ii)

Key- node support values

- Posterior probabilities 1.0 in 3x MrBayes consensus trees (GTR, Jones, WAG)
- Posterior probabilities > 0.8 in all MrBayes trees

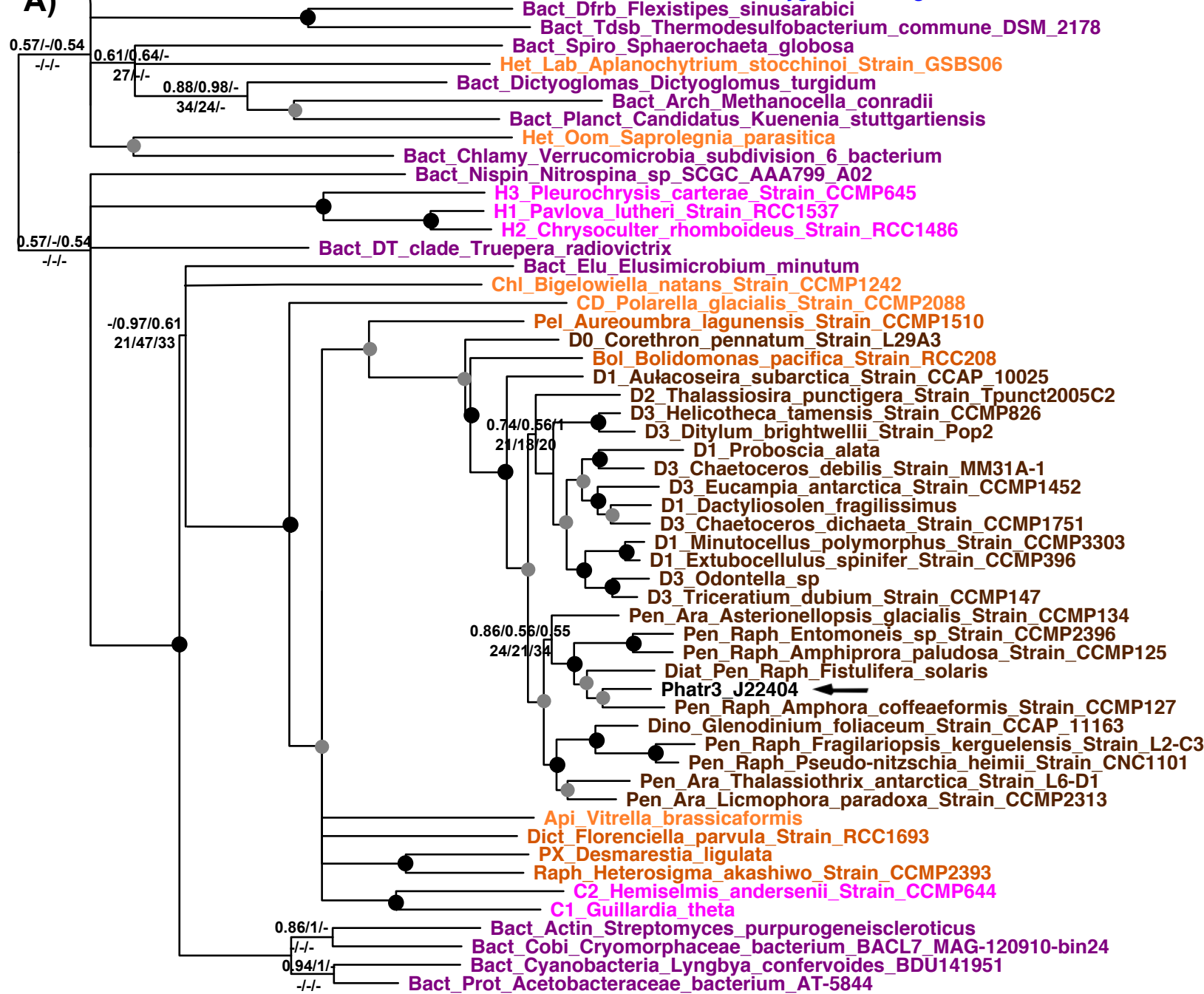
x/y/z MrBayes: GTR, Jones, WAG
a/b/c RAxML: GTR, JTT, WAG (used for all remaining nodes)

Key- taxon labels

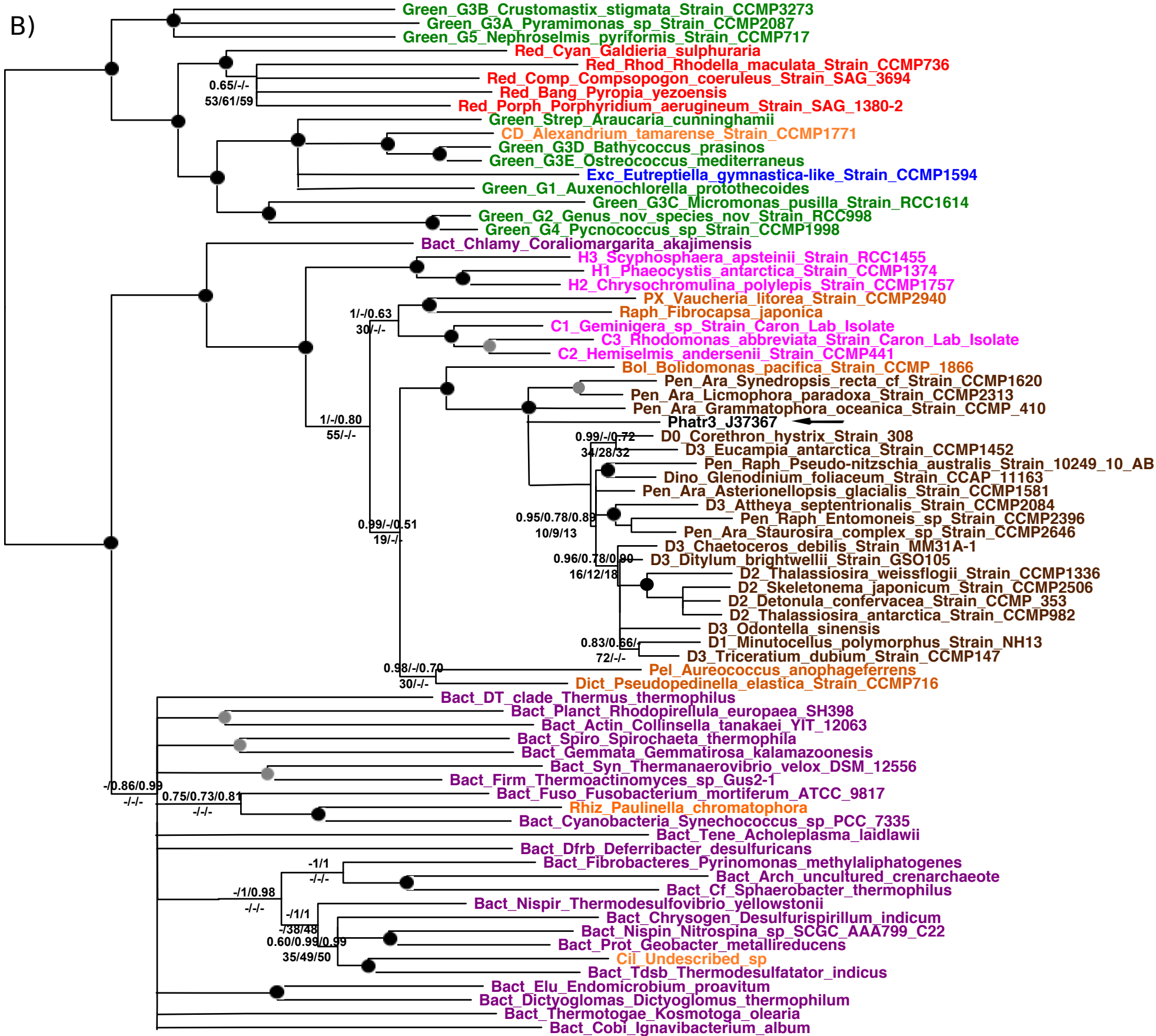
- Diatoms
- Other stramenopiles
- Other SAR
- CCTH
- Red algae
- Green lineages and glaucophytes
- Amorphea
- Prokaryotes
- Viruses

Other_Het_Exc_Stygamoeba_regulata_Strain_BSH-02190019

A)



B)



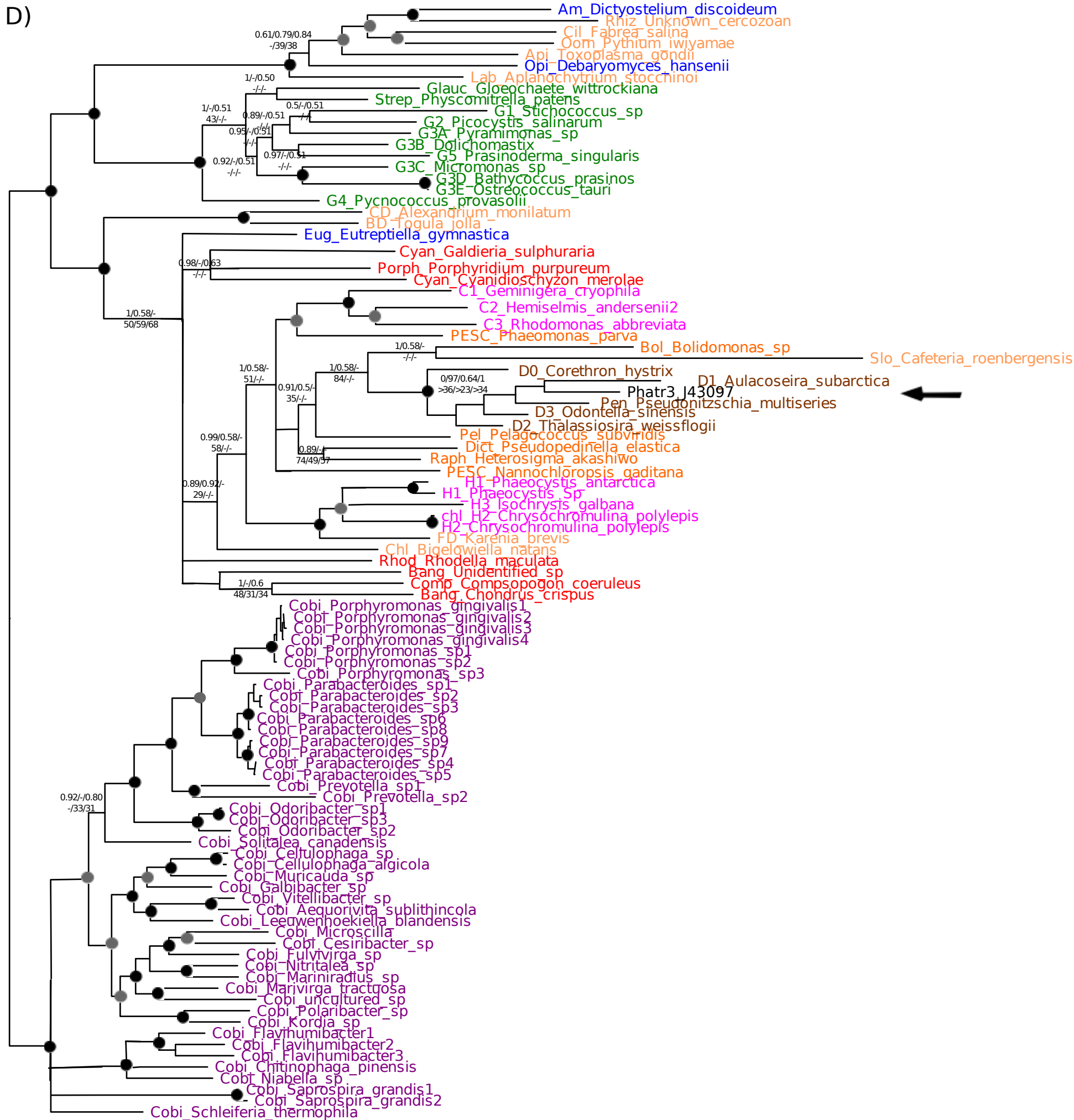
0.2

c)



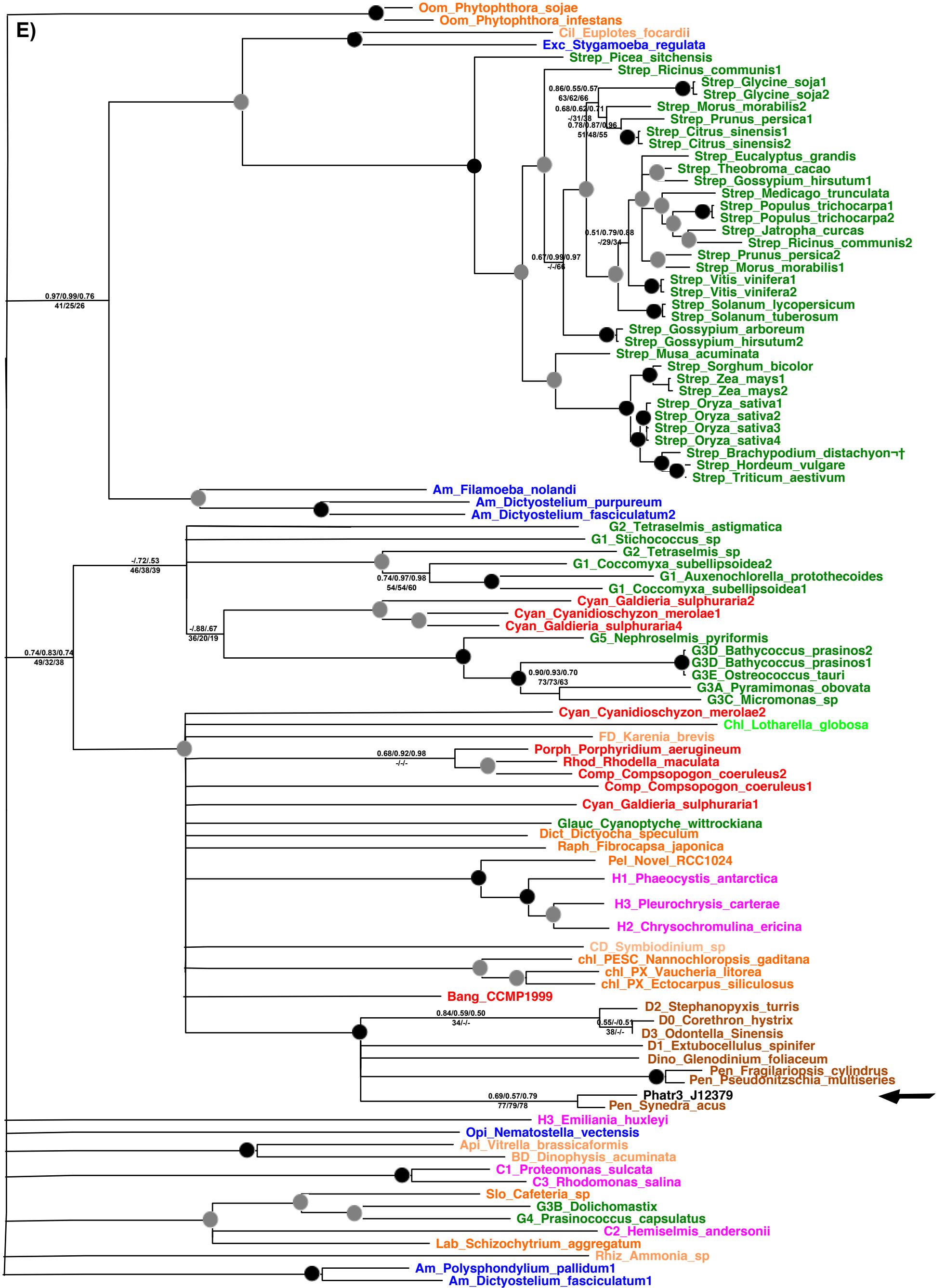
0.2

D)



0.2

E)





0.2



